Research Square

Preprints are preliminary reports that have not undergone peer review.
They should not be considered conclusive, used to inform clinical practice,
or referenced by the media as validated information.

Delayed psilocybin treatment after repeated mild traumatic brain injury recovers chronic behavioural deficits, reduces microglial density, and enhances hippocampal neurogenesis in rats

Sandy Shultz

sandy.shultz@monash.edu

Monash University https://orcid.org/0000-0002-2525-8775

Josh Allen

Grace O'Regan

https://orcid.org/0009-0007-5855-9439

Justin Brand

https://orcid.org/0009-0005-4927-8438

Paul Liknaitzky

Terrence O'Brien

Brian Christie

University of Victoria https://orcid.org/0000-0002-6830-0160

Stuart McDonald

Article

Keywords: Concussion, persistent-post concussion symptoms, chronic traumatic encephalopathy, neuroinflammation, neuroplasticity, psychedelic-assisted therapy

Posted Date: February 23rd, 2026

DOI: https://doi.org/10.21203/rs.3.rs-8555503/v1

License: This work is licensed under a Creative Commons Attribution 4.0 International License. Read Full License

Additional Declarations: The authors have declared there is **NO** conflict of interest to disclose

Abstract

Repeated mild traumatic brain injury (RmTBI) can produce lasting cognitive, emotional, and social deficits (e.g., persistent post-concussion symptoms; PPCS). Despite the prevalence of RmTBI in sports, military, and domestic violence settings, effective treatments to alleviate the neurological consequences of RmTBI remain limited. Psilocybin, a serotonergic psychedelic, can enhance neuroplasticity and reduce neuroinflammation and has shown efficacy in psychiatric conditions that share overlapping pathophysiological and symptomatic features with RmTBI and PPCS. Here we examined whether delayed administration of psilocybin after RmTBI could improve long-term recovery in rats. Adult male rats received either five mTBIs delivered once daily via a lateral impactor or underwent sham procedures. After an 8-week recovery period, rats were administered psilocybin (1 mg/kg, i.p.) or saline. Behavioural testing began 24 hours later to evaluate psilocybin's potential therapeutic effects. Afterwards, rats were perfused for immunohistochemical analysis of Cd11b and doublecortin to assess the density and morphology of microglia and newborn neurons, respectively, in the dorsal dentate gyrus. RmTBI produced persistent behavioural deficits across affective, social, and cognitive domains. Psilocybin treatment reversed several of these alterations, exhibiting antidepressant-like effects in the forced swim and sucrose preference tests, promoting pro-social behaviour, and increasing nociceptive thresholds in the hot plate test. Psilocybin also partially recovered RmTBI-induced increases in microglial density and, while RmTBI had minimal impact on the number of newborn neurons, psilocybin increased their abundance and enhanced their dendritic complexity. These results support the potential of psilocybin as a novel intervention for the enduring consequences of RmTBI.

1. Introduction

Mild traumatic brain injury (mTBI; e.g., concussion), is a major public health concern associated with persistent cognitive, emotional, and behavioural impairments [1, 2]. Repeated mTBI (RmTBI), which commonly occurs in contact sports, military settings, falls, and intimate partner violence, confers an elevated risk of persistent post-concussion symptoms (PPCS) and increases vulnerability to psychiatric and neurodegenerative and disorders, including depression, anxiety, and dementia [3–6]. Despite these substantial long-term consequences, effective treatments that promote recovery in the chronic stage remain limited.

RmTBI can induce a sustained neuroinflammatory response marked by chronic microglial activation – associated with a retraction of branches and enlarged soma size – which contributes to secondary injury cascades and long-term neural dysfunction [7–9]. In parallel, RmTBI may also disrupt neuroplasticity [10], including adult hippocampal neurogenesis, leading to aberrant proliferation, survival, and maturation of newborn neurons in the dentate gyrus [11–13]. Because neurogenesis is tightly regulated by microglial phagocytosis, trophic support, and inflammatory signalling [14, 15], chronic microglial dysregulation likely amplifies neurogenic impairments. Thus, interventions that restore both microglial function and neuroplasticity – including neurogenesis – may offer a complementary avenue to support recovery.

Psilocybin, a serotonergic psychedelic, has demonstrated clinical efficacy in disorders such as depression, anxiety, and post-traumatic stress disorder, conditions that share symptoms, as well as impairments in neuroplasticity and elevated neuroinflammation, with RmTBI [16–18]. Evidence also suggests that psilocybin may improve cognition [19, 20], reduce headache burden and chronic pain [21–24], and decrease substance use [25–27]. Psilocybin's therapeutic effects are thought to arise primarily through activation of 5-HT_{2A} and TrkB receptors, which engage intracellular pathways that promote neuroplasticity, including dendritic growth, spinogenesis, and synaptic strengthening [28–35]. Given the plasticity of adult hippocampal neurogenesis, these mechanisms support a role for psilocybin in promoting neuron generation and maturation. Consistent with this possibility, preclinical work suggests that psilocybin exerts dose-dependent effects on neurogenesis, although evidence remains limited – particularly in the context of brain injury [36]. Additionally, psilocybin treatment has been shown to reduce neuroinflammation, lower pro-inflammatory cytokine expression and oxidative stress, modulate microglial activation [37–40], and extend cellular lifespan [41]. Together, these complementary effects position psilocybin as a promising candidate for restoring neuroimmune balance and improving long-term outcomes following RmTBI. However, its therapeutic potential in this domain remains largely unexplored.

To address this knowledge gap, we examined whether delayed administration of psilocybin after RmTBI could improve long-term recovery in a rat model.

2. Methods

2.1 Animal husbandry

Male Sprague-Dawley rats (N=48), aged 6 weeks, were obtained from the Alfred Medical and Education Precinct Animal Services (AMREP) in Melbourne, Australia, and housed in groups of three under a 12 hour light-dark cycle with ad libitum food and water. Bedding was changed weekly. After a 7-day habituation and 1 week of handling, experimental procedures began. All procedures were approved by the AMREP Ethics Committee (E/8029/2021/M) and conducted in accordance with the Australian National Health and Medical Research Council's Code of Practice for the Care and Use of Animals for Scientific Purposes. The experimental design is depicted in Figure 1A.

2.2 Repeated mild traumatic brain injury

To model RmTBI, rats were subjected to a lateral impact once a day for five consecutive days, or a sham procedure, as previously described [42, 43]. First, the rats were lightly anesthetized with 5% isoflurane inhalation (until non-responsive to toe-pinch; ~ 90 seconds) and placed chest down on a Teflon® board, with the left temporal region of its head positioned against a helmet-like aluminium plate (30 × 13 × 3 mm^3) that was facing the impactor. The impactor used pneumatic pressure to propel a 50-gram weight at the plate at an average speed of 11 m/s. The sham procedure was identical but did not include the weight being propelled. After the procedure, the rat was placed into a clean cage and latencies to toe pinch and self-righting were measured.

2.3 Acute behavioural testing

Sensorimotor functioning

Five minutes after each injury, we assessed the rat's startle response and their ability to traverse a beam and hold on to a rotating beam [44–46]. Each test was scored 0-3, where 0 indicated poor performance (no sound response, inability to cross the beam within 10 seconds, or failure to hold after one rotation) and 3 indicated superior performance (sound response, beam crossing with ≤1 slip within 10 seconds, and remaining on the beam after four rotations).

Beam-walk

Sensorimotor function was evaluated with a beam-walk test 1-hour, 1-day, and 2-days post-final injury [47, 48]. Initially, rats underwent beam training the day before the first injury, completing 5 trials on a 100 cm long × 4 cm wide beam, then 5 trials on a narrower 100 cm long × 2 cm beam. Testing consisted of 10 trials on the 2 cm beam, with a 60 second limit per trial. Traversal time, slips, and falls were recorded, and rats that fell or failed to hold the beam were assigned 60 seconds for that trial.

T-maze

Spatial memory was evaluated 3 days after the final injury, as previously described [46]. This test relies on the rats' natural preference for novel stimuli. Rats explored a T-shaped arena with 2 accessible arms for 10 minutes, then returned 1 hour later to explore all 3 arms for 5 minutes. TopScan™ software (v3.0; Clever Sys., USA) quantified time spent and entries into each arm.Additionally, the pattern of arm alternations was recorded to assess spatial working memory using the following formula: Spontaneous alternation % = (number of complete sequences ÷ (total number of alternations – 2) × 100). For example, in the following pattern of arm visits, the underlined arms are the start of complete non-repeating 3-arm sequences: Start→Familiar→Novel→Familiar→Start→Novel.

2.4 Psilocybin administration

After an 8-week recovery period – selected to model the chronic phase of injury and align with the clinical timeframe for PPCS [49] – the rats received an intraperitoneal injection of either psilocybin (1 mg/kg, dissolved in saline at a volume of 1 mg/ml) or saline control. This dose of psilocybin was chosen based on previous work demonstrating its positive behavioural and neurochemical effects in various rodent models and is thought to be equivalent to a clinical high dose [32, 34, 43, 50]. Psilocybin induces a transient, 5-HT_{2A} receptor-dependent head-twitch response in rodents that peaks 6-8 minutes post-administration [34, 51]. Accordingly, to confirm successful dosing, rats were placed individually into a bedded cage immediately after psilocybin or saline treatment, and the number of head-twitches were recorded for 15 minutes [43]. After an hour, the rats were returned to their original home-cage.

2.5 Chronic behavioural testing

Beginning 24 hours after psilocybin administration, rats underwent behavioural tests assessing anxiety- and depression-like behaviour, motor function, pain sensitivity, cognition, and sociability. All tests were conducted and scored by researchers blinded to treatment. Where possible, we utilized video tracking software (TopScan^{TM} 3.0; Clever Sys., Inc., USA) to automatically quantify relevant metrics, minimizing experimenter bias.

Elevated-plus maze

Rats were tested in the elevated-plus maze to make inferences about anxiety-like behaviour 24 hours after treatment [44]. Rats explored a 50 cm by 10 cm "+"-shaped arena with two of the opposing arms open and two enclosed arms for 5 min, while time spent and entries into each arm were recorded.

Forced swim

The forced swim test, which assesses coping responses to inescapable stress, is widely used as a standard assay of antidepressant-like efficacy [52]. Rats were first placed in a 24 cm-diameter, 40 cm-high cylinder filled with 30 cm of water (23–25 °C) for 10 minutes to familiarize them with the inescapable stress. Twenty-four hours later, rats were reintroduced for 5 minutes while swimming, climbing/struggling, and immobility were manually scored from video recordings.

Hot and cold plate

Pain sensitivity was assessed using a hot/cold plate test [43]. Rats were habituated to the enclosed temperature-controlled plate the day before psilocybin. Four days post-treatment, latency to paw lick or jump was recorded on a 52 °C plate, then repeated 1 hour later on a 2 °C plate. A maximum time of 2 minutes was allowed for each trial. Shorter latencies indicated increased pain sensitivity

Open field

Five days post-psilocybin, the open field test assessed exploratory behaviour as an indicator of anxiety [47, 48]. Rats were placed in the centre of a 100 cm-diameter well-lit arena for 5 min, with less time spent in the central 66 cm zone indicating higher anxiety-like behaviour.

T-maze

Spatial memory was re-assessed using the T-maze test 6-days post-psilocybin treatment, following the same procedure as described for the acute T-maze test.

Rotarod

The rotarod test, conducted 7 days post-psilocybin, assessed motor function [43]. Rats were habituated at 4 rpm for 2 min, followed by two trials with speed increasing from 4-40 rpm over 5 minutes. The test session included another 3 consecutive trials, with speed progressively increasing from 4-40 rpm within the allotted 5-minute duration, with fall time recorded by a sensor. Any rat remaining on the rotarod for 5 minutes was returned to their home cage. Longer latencies indicate better motor performance.

Social interaction

The social interaction test, conducted 8 days post-treatment, assessed sociability based on rats' preference for novel over familiar conspecifics [53]. Rats explored a three-chamber arena (100 × 100 × 50 cm) with stimulus rats confined in mesh cages in the outer chambers. The test included a 10 minute habituation, followed by two 10 minute trials: trial 1 measured preference for a single stimulus rat, and trial 2 assessed interaction with a novel rat in the previously empty chamber. Time spent in each chamber and the "sniff zone" indicated social behaviour.

Water maze

Spatial cognition was assessed using the water maze 9–10 days post-treatment [42, 53]. Rats navigated a 163 cm-diameter pool (26–28 °C) to locate a hidden platform, guided by four visible cues positioned around the pool's perimeter at north, east, south, and west. During acquisition (day 1), each rat completed 10 trials with randomized start points; latency to find the platform was recorded. Rats failing to find the platform within 60 seconds were guided to it for 15 seconds. A reversal session 24 hours later relocated the platform to the opposite quadrant, with latency again measured as an index of learning and memory.

Sucrose preference

The sucrose preference test assessed anhedonia-like behaviour [54]. Throughout the study as the rats were housed in groups of 3, they had access to two water bottles. The day before the test, they were given two bottles of 1% sucrose for 24 hours. On testing day, 11 days after treatment, rats were singly housed with one water bottle and one 1% sucrose bottle for 24 hours, with positions switched after 12 hours to control for side preference. Sucrose consumption as a percentage of total fluid intake was calculated, with reduced preference indicating anhedonia-like behaviour.

2.6 Tissue preparation and immunohistochemical analyses

After behavioural testing, the rats were transcardially perfused with ~450 ml of ice-cold 0.1 M phosphate buffer (PB; pH 7.4) followed by ~450 ml of ice-cold 4% (w/v) paraformaldehyde in 0.1 M PB (pH 7.4). The brains were then removed and post-fixed in 4% paraformaldehyde (w/v) for 48 hours at 4°C. Thereafter, the brains were suspended in a 30% sucrose solution for 72 hours and then suspended in OCT and flash frozen with liquid nitrogen before being sectioned at a thickness of 40 μm using a cryostat.

Microglial and adult-born neurons were assessed by immunohistochemical detection of Cd11b and doublecortin (DCX), respectively, in the dorsal hippocampus using methods described previously [55]. Every 6^{th} tissue section (i.e., spaced 240 μm apart) was processed for immunohistochemistry. Sections underwent antigen retrieval in sodium citrate buffer (pH 6.0) at 85 °C for 30 minutes, then incubated for 24 hours at room temperature with either a mouse anti-CD11b primary antibody (1:500; Millipore, USA) or a rabbit anti-DCX primary antibody (1:1000; Cell Signaling, Danvers, MA), both diluted in a blocking solution consisting of Tris-buffered saline, 0.5% Triton X-100, 1% bovine serum albumin, and 5% normal horse serum for CD11b staining or normal goat serum for DCX staining. Endogenous peroxidase activity was quenched with 10% H_2O_2 for 30 minutes, followed by a 2-hour incubation with either a biotinylated horse anti-mouse

(1:500; Sigma-Aldrich) or goat anti-rabbit secondary antibody (1:500; Vector Laboratories) in blocking solution. Sections were then treated with avidin-biotin complex (ABC; 1:500; Vector Laboratories) for 1 hour and visualized using 0.025% diaminobenzidine with 4.167% nickel sulphate and 0.002% H_2O_2 in 0.175 M sodium acetate buffer (pH 6.8). Finally, sections were mounted onto glass slides, air-dried overnight, dehydrated through graded ethanol (70%, 95%, and 100%), cleared in xylene, and coverslipped using Permount mounting medium.

2.7 Cd11b- and DCX-positive cell counts and morphological analyses

All quantification was conducted by an experimenter blinded to experimental conditions using an Olympus BX51 microscope equipped with a motorized stage and linked to a computerized image analysis system (Stereo Investigator, MicroBrightField). Measurements were obtained from both hemispheres across four tissue sections at 40× magnification.

The estimated number of CD11b-positive microglia was determined using unbiased stereology with a modified optical fractionator method to minimize oversampling, as previously described [43]. The total cell count (Ntotal) was calculated using the following formula:

Ntotal: $\Sigma Q- \times 1 / ssf \times A(x, y\ step) / a(frame) \times t/h$,

where ΣQ− is the number of counted cells; ssf is the section sampling fraction (1 in 6); A(x,y step) is the area associated with each x,y movement (90000 μm^2); a(frame) is the area of the counting frame (7500 μm^2); t is the weighted average section thickness; and h is the height of the dissector (30 μm). A guard zone of 4 μm was used to avoid counting sectioning artefacts.

DCX-positive neurons were quantified using a profile-based counting approach. Immunolabeled neurons were manually counted within the granule cell layer and subgranular zone. Profile counting involved identifying and counting only DCX-positive neurons with a clearly stained soma to minimize overestimation from dendritic fragments or partial profiles. Neuron counts were area-normalized and expressed as a percentage change relative to the sham/saline group.

The morphology of 10 randomly selected CD11b- and DCX-positive cells per rat were traced using Neurolucida software (MicroBrightField) at 100× magnification with oil immersion. Cells were selected based on the presence of a clearly defined soma, well-resolved processes or intact primary dendrite, and minimal overlap with neighbouring cells. Quantitative analyses of the soma and process branching parameters were performed using NeuroExplorer software (MicroBrightField). Process complexity was further assessed using Sholl analysis, in which concentric circles spaced at 10 μm intervals were centered on the soma of each traced cell. This approach enabled quantification of morphological features including process intersections, branching nodes, terminal endings, and cumulative process length within each radial segment.

2.8 Statistical analyses

An a priori power analysis indicated that a minimum of 10 rats per group would be required to detect a large effect size (Cohen's $f = 0.4$) across four groups ($k = 4$), with a significance level of $\alpha = 0.05$ and a desired statistical power of 80% ($1 - \beta = 0.8$). To ensure adequate power and account for potential attrition, we included 12 rats per group. This sample size aligns with previous psilocybin studies in rodents that have demonstrated significant effects using comparable or even smaller group sizes [32, 34, 56].

Bodyweight, measured throughout the experiment, was analysed with a repeated measures ANOVA, with injury as the between-subject factor (sham vs RmTBI) and time (week) as the within-subject factor.

Acute injury and behavioural data were analysed using independent t-tests or Mann–Whitney U tests, depending on the outcome of the Shapiro-Wilk test for normality, to compare sham and RmTBI groups.

Chronic behavioural and neurobiological data was analysed with two-way ANOVAs, with injury (sham vs RmTBI) and treatment (saline vs psilocybin) as factors. Tukey multiple comparison post-hoc tests were used if significant main or interaction effects were observed at $p<0.05$. Non-normally distributed data were analysed using Kruskal-Wallis tests, followed by Dunn's post-hoc tests where appropriate ($p<0.05$).

3. Results

3.1 Bodyweight and acute injury severity measures

A repeated measures ANOVA analysis of body weight (Figure 1B) revealed a significant main effect of time [$F(3.010, 138.444)=929.996$, $p<0.001$], with both injury groups gaining weight over the course of the experiment. However, there was no significant main effect of RmTBI [$F(1, 46)=0.610$, $p=0.439$], nor a significant time × RmTBI interaction [$F(3.010, 138.444)=0.849$, $p=0.470$].

To confirm injury induction, we demonstrated that RmTBI rats took longer to self-right after each injury (Figure 1C; day 1: $t(46)=-7.090$, $p<0.001$; day 2: $t(46)=-8.128$, $p<0.001$; day 3: $t(46)=-11.879$, $p<0.001$; day 4: $t(46)=-12.841$, $p<0.001$; day 5: $t(46)=-12.050$, $p<0.001$) and exhibited significantly impaired performance on sensorimotor assessments conducted five minutes after each injury (Figure 1D; day 1: $U=-6.051$, $p<0.001$; day 2: $U=-5.801$, $p<0.001$; day 3: $U=-6.052$, $p<0.001$; day 4: $U=-6.052$, $p<0.001$; day 5: $U=-6.071$, $p<0.001$).

Additionally, RmTBI rats took significantly longer to traverse a beam 1-hour [$t(46)=-4.074$, $p<0.001$], 1-day [$t(46)=-4.202$, $p<0.001$], and 2-days [$t(46)=-3.058$, $p=0.004$] post-final injury (Figure 1E). RmTBI also led to a greater number of slips and falls at the 1-hour ($U=-4.736$, $p<0.001$) and 1-day ($U=-3.102$, $p=0.002$) timepoints, although performance returned to baseline by 2 days post-injury ($U=-1.620$, $p=0.105$).

As well, rats subjected to RmTBI spent significantly less time in the T-maze novel arm [$t(46)=3.539$, $p=0.001$], and significantly more time in the familiar arm [$t(46)=-2.300$, $p=0.026$], compared to sham controls 3-days post-injury (Figure 1F). Time spent in the start arm was also reduced in RmTBI rats, approaching statistical significance [$t(46)=2.008$, $p=0.051$]. However, RmTBI had no significant effect on the number of entries into the novel ($U=-1.614$, $p=0.107$), start ($U=-1.804$, $p=0.071$), or familiar ($U=-1.334$, $p=0.182$) arms.

Notably, there were no significant differences in acute injury severity measures between the psilocybin or saline treatment groups that were assigned thereafter, confirming comparable baseline impairment prior to intervention.

[insert Figure 1 here]

3.2 Psilocybin improved behavioral outcomes

Head-twitch response

Head-twitch behaviour, a 5-HT_{2A} receptor-mediated response to psilocybin [43], was assessed following treatment to confirm successful drug delivery (Figure 2A). A Kruskal-Wallis test revealed a significant effect of group ($H=39.410$, $p<0.001$), and Dunn's post-hoc tests confirmed that psilocybin-treated rats, regardless of injury group, exhibited significantly more head twitches compared to their respective saline-treated counterparts ($p<0.001$).

Elevated plus-maze

Analysis of elevated plus-maze performance revealed no significant main effects of RmTBI [$F(3, 44)=1.760$, $p=0.191$], psilocybin treatment [$F(3, 44)=1.138$, $p=0.292$], or their interaction [$F(3, 44)=0.866$, $p=0.357$] on time spent in the open arms (Figure 2B). Similarly, the number of entries into the open arms was not significantly affected by RmTBI [$F(3, 44)=1.140$, $p=0.291$], psilocybin treatment [$F(3, 44)=1.993$, $p=0.324$], or their interaction [$F(3, 44)=0.324$, $p=0.572$].

Forced swim

There was a significant main effect of RmTBI [$F(3, 44)=16.339$, $p<0.001$] and psilocybin [$F(3, 44)=10.870$, $p=0.002$] on forced swim immobility (Figure 2C), but no significant RmTBI × psilocybin interaction [$F(3, 44)=2.335$, $p=0.134$]. Tukey post-hoc analyses revealed that RmTBI/saline rats were immobile for significantly longer periods than both sham/saline ($p=0.002$) and RmTBI/psilocybin ($p=0.007$) rats.

Additionally, there was a significant RmTBI effect on latency to first immobility [$F(3, 44)=22.942$, $p<0.001$], but no psilocybin [$F(3, 44)=2.696$, $p=0.108$] or interaction effect [$F(3, 44)=1.415$, $p=0.241$]. Tukey post-hoc comparisons showed that RmTBI/saline rats became immobile significantly faster than sham/saline rats ($p=0.001$) but not significantly faster than RmTBI/psilocybin rats ($p=0.132$).

Hot/cold plate

Reaction time in the hot plate test (Figure 2D) was unaffected by RmTBI [$F(3, 44)=0.497$, $p=0.484$]. However, a significant main effect of psilocybin treatment was observed [$F(3, 44)=4.766$, $p=0.034$], along with a significant RmTBI × psilocybin interaction [$F(3, 44)=5.787$, $p=0.020$]. Tukey post-hoc analyses revealed that psilocybin significantly increased reaction time in RmTBI rats ($p=0.012$). In the cold plate test (Figure 2E), a Kruskal-Wallis test showed no significant group differences in reaction time ($H=6.508$, $p=0.089$).

Open field

There were no significant effects of RmTBI [F(3, 44)=0.665, p=0.419], psilocybin [F(3, 44)=1.853, p=0.180], or their interaction [F(3, 44)=0.046, p=0.831] on time spent in the centre of the open field arena (Figure 2F). Similar non-significant effects were observed for the number of entries into the centre (RmTBI: [F(3, 44)=0.624, p=0.434]; psilocybin: [F(3, 44)=1.670, p=0.203]: RmTBI x psilocybin: [F(3, 44)=0.253, p=0.618]) and total distance travelled (RmTBI: [F(3, 44)=0.321, p=0.574]; psilocybin: [F(3, 44)=0.005, p=0.946]: RmTBI x psilocybin: [F(3, 44)=0.004, p=0.949]).

T-maze chronic

There were no significant main effects of RmTBI [F(3, 44)=0.001, p=0.981], psilocybin [F(3, 44)=0.785, p=0.380], or their interaction [F(3, 44)=1.737, p=0.194] on percentage of time spent in the novel arm (Figure 2G).

Rotarod

There was a significant main effect of RmTBI [F(3, 44)=4.241, p=0.045] on motor function in the Rotarod test (Figure 2H), but no effect of psilocybin [F(3, 44)=0.982, p=0.327] or their interaction [F(3, 44)=1.492, p=0.228]. Tukey post-hoc analyses revealed no significant individual group differences.

Social interaction

In trial 1 of the social interaction test (Figure 2I), where the subject rat could interact with a single conspecific, there were no significant main effects of RmTBI [F(3, 44)=1.886, p=0.177], psilocybin [F(3, 44)=0.001, p=0.990], or their interaction [F(3, 44)=2.828, p=0.100] on social preference. However, in trial 2, which assessed novel rat preference, significant main effects were observed for RmTBI [F(3, 44)=4.161, p=0.047], psilocybin [F(3, 44)=7.145, p=0.011], and their interaction [F(3, 44)=5.976, p=0.019]. Tukey post-hoc tests revealed that RmTBI/saline rats showed significantly reduced preference for the novel rat compared to both sham/saline (p=0.014) and RmTBI/psilocybin (p=0.004) rats.

Water maze

In the acquisition phase of the water maze test (Figure 2J), Kruskal-Wallis tests revealed a significant effect of group in trial 6 (H=8.613, p=0.035), although post-hoc testing revealed no significant group differences.

In the reversal phase, Kruskal-Wallis tests revealed a significant effect of group in trial 2 (H=10.018, p=0.018), 7 (H=14.178, p=0.003), 9 (H=12.054, p=0.007), and 10 (H=9.413, p=0.024). Dunn's post-hoc testing revealed that RmTBI/saline rats took significantly longer to locate the hidden platform than sham/saline rats in trial 9 (p=0.022). Similarly, RmTBI/psilocybin rats were slower than sham/psilocybin rats in trial 7 (p=0.027).

Sucrose preference

There was a significant effect of RmTBI [F(3, 44)=6.210, p=0.017] on sucrose preference (Figure 2K), but not psilocybin [F(3, 44)=2.700, p=0.108]. The interaction effect of RmTBI x psilocybin approached statistical

significance [F(3, 44)=4.062, p=0.050]. Tukey post-hoc analyses revealed that sham/saline rats had an increased preference for sucrose than sham/saline rats (p=0.014).

[insert Figure 2 here]

3.3 The effect of RmTBI and psilocybin on Cd11b-positive cell counts and morphology

Statistical data for Cd11b-positive cell counts and morphological measurements are presented in Table 1. Therefore, below we report detailed statistics only for post-hoc group comparisons. Sham/saline rats had an increased number of Cd11b-positive cells in the hippocampal molecular layer compared to RmTBI/saline rats (p=0.034; Figure 3A). There were no significant main effects of RmTBI, psilocybin treatment, or their interaction on soma perimeter and roundness, but psilocybin significantly reduced soma area in RmTBI rats (p=0.046; Figure 3B). Although RmTBI produced significant main effects on process quantity, number of process endings, total process length, and process surface area, these effects did not translate into significant pairwise differences between groups in post-hoc testing (Figure 3C).

Sholl analyses were conducted to further assess microglial process arborization across radial distance segments. RmTBI significantly reduced the number of process nodes within 20 μm of the soma in saline-treated rats (p=0.007), as well as intersections within 10 μm of the soma in psilocybin-treated rats (p=0.044; Figure 3D).

[insert Figure 3 here]

3.4 The effect of RmTBI and psilocybin on DCX-positive neuron counts and morphology

Statistical data for DCX-positive neuron counts and morphological measurements are presented in Table 2. Therefore, below we report detailed statistics only for post-hoc group comparisons. Despite a significant main effect of psilocybin on DCX-positive neuron profile counts (Figure 4A), there were no significant post-hoc group differences. There were no significant main effects of RmTBI, psilocybin treatment, or their interaction on soma area, perimeter, and roundness measurements (Figure 4B). However, a Kruskal-Wallis test revealed a significant group effect on dendritic complexity (Figure 4C), with post-hoc analyses revealing that psilocybin significantly increased dendritic complexity in RmTBI rats (p=0.032). Although there was a significant main effect of psilocybin on dendritic surface area and total length – with psilocybin increasing these measurements – post-hoc comparisons did not reveal significant differences between individual groups.

Sholl analyses were conducted to further assess the complexity of dendritic arborization across radial distance segments. Although there was no RmTBI main effects on Sholl measurements, there was a significant main effect of psilocybin on dendritic length in the 90-110, 110-130, and 150-170 μm segments; dendritic nodes in the 90-110 and 110-130 μm segments; dendritic endings in the 110-130 and 170-190 μm segments; and the number of intersections in the 90-110 μm and 110-130 μm segments (Figure 4D). However, post-hoc comparisons did not reveal statistically significant differences between individual groups. There was also a significant interaction effect of RmTBI x psilocybin treatment on nodes in the 30-50 and 70-90 μm segments, but no post-hoc individual group differences.

[insert Figure 4 here]

4. Discussion

This study investigated the therapeutic potential of psilocybin on long-term behaviour, microglial dynamics, and hippocampal neurogenesis following RmTBI in rats. We found that psilocybin: 1) produced antidepressant-like and pro-social effects; 2) decreased hippocampal microglial density; and 3) enhanced hippocampal neurogenesis.

To model RmTBI, we employed a lateral impact paradigm [44, 48] developed to mirror the biomechanics of sports-related concussions [57]. We then allowed an 8-week recovery period designed to reflect the chronic phase of injury and mirror the clinical course of PPCS. Thereafter, psilocybin was administered and elicited an acute head-twitch response, a hallmark of 5-HT_{2A} receptor activation [34]. Subsequently, we showed that psilocybin reversed RmTBI-induced increases in forced swim test immobility and partially restored reductions in sucrose preference, indicating antidepressant-like effects. Psilocybin also restored RmTBI-induced reductions in novel rat preference in the social test. Social impairments following RmTBI are associated with alterations in 5-HT_{2A} receptor activity, and agonising this receptor mitigates these deficits [58]. Our findings are promising since depression symptoms, including anhedonia and social withdrawal, are commonly reported after mTBI and are difficult to treat [59–62]. Cognitive deficits in the water maze induced by RmTBI were not reversed by psilocybin. Neither RmTBI nor psilocybin produced chronic behavioural changes in the elevated plus-maze, open field, T-maze, or rotarod tests, suggesting that alternative injury models, recovery timepoints, dosing regimens, or more sensitive outcome measures may be required to determine whether psilocybin improves anxiety-like behaviour or sensorimotor performance following RmTBI. Indeed, psilocybin has demonstrated anxiolytic properties in previous preclinical [50, 63] and clinical studies [64–68], though clinical trials typically involve psychotherapy and often multiple dosing sessions.

Hippocampal microglial density was increased after RmTBI in rats treated with saline, but not those treated with psilocybin. Psilocybin also reduced microglial soma area, consistent with a shift toward a more surveillant, less inflammatory phenotype [69]. These findings align with our recent work showing reduced hippocampal microglial density following psilocybin administration four months after RmTBI combined with hypoxic non-fatal strangulation in a female rat model of intimate partner violence [43]. Excessive microglial activation is known to amplify chronic neuroinflammatory signalling and synaptic dysfunction [70]. Thus, normalizing microglial populations may, in turn, reduce neuroinflammation and promote neuronal plasticity and circuit repair. Microglial changes likely involve 5-HT_{2A} receptor activation [38, 71, 72]; however, future studies should examine serotonergic, neuroimmune, and plasticity-related pathways to clarify the underlying mechanisms.

Rodent studies demonstrate that adult-born dentate neurons are critical for stress resilience, emotional regulation, and adaptive behaviour [73–75]. Disruption of their survival, maturation, or functional integration – as observed following chronic RmTBI – is associated with depression-like phenotypes, including reward sensitivity, social withdrawal, cognitive deficits, and maladaptive coping [11, 76]. Psilocybin enhanced

hippocampal neurogenesis, evidenced by more DCX-positive neurons and greater dendritic complexity. Thus, psilocybin's behavioural effects may arise from broader hippocampal plasticity, with recovery of neurogenic output after RmTBI representing one contributing mechanism. Notably, our cell counts differ from prior reports showing reduced newborn neurons following the same dose of psilocybin, whereas a lower dose (0.1 mg/kg) enhanced neurogenesis, highlighting the potential to optimize dosing for maximal benefit [36]. However, methodological differences, including species, age, disease model, histological markers, and post-administration interval, may account for these discrepancies.

Given psilocybin's complex polypharmacology, identifying the precise mechanisms related to its neuroplastogenic and behavioural effects is challenging. These outcomes may involve several pathways, including activation of 5-HT_{2A} and other serotonin receptors, BDNF release and TrkB allosteric modulation, and mTOR-dependent cascades [28, 29, 31, 43]. Immature dentate neurons minimally express 5-HT_{2A} receptors, which are mainly localized to cortical pyramidal neurons and GABAergic interneurons [77]. This suggests psilocybin acts indirectly via network plasticity, modulation of the neurogenic niche, or shifts in inflammatory tone. Other psychedelics like NN-DMT and 5-MeO-DMT also stimulate neurogenesis [78, 79], suggesting the involvement of 5-HT_{2A} receptors, but these effects could be mediated by activating sigma-1 receptors [80], which psilocybin does not target.

This study has several limitations. First, the cellular mechanisms underlying the psilocybin's effects remain unexamined, yet are crucial for understanding its behavioural, anti-inflammatory, and neuroplastic actions. Notably, although psilocybin reduced microglial density, cell counts alone do not confirm anti-inflammatory activity, which depends on dynamic cytokine and chemokine signalling. Second, neurogenesis was assessed using DCX alone, which does not fully capture the entire neurogenic process. Inclusion of additional markers for proliferation and maturation (e.g., Ki-67, BrdU, NeuN, calretinin) would help determine where psilocybin acts along the neurogenic timeline and clarify its effects on neuronal survival, maturation, and integration, providing deeper insight into psilocybin's therapeutic potential and limitations in supporting long-term neuroplasticity. Third, intervention timing remains understudied. While psilocybin was administered in the chronic phase to model PPCS, the efficacy of earlier or alternative dosing schedules is unknown, highlighting the need to define optimal therapeutic windows across injury stages. Lastly, our findings may not generalize to females, given sex differences in mTBI outcomes, neuroplasticity, and serotonergic signalling [76, 81–88]. However, male rats were selected to reflect the higher incidence of sports-related concussions in men [49], while our previous work examined psilocybin's effects in a female model reflecting intimate partner violence-related brain trauma, which disproportionately affects women [43]. Clarifying psilocybin's effects across sex-relevant and clinically distinct forms of brain injury is essential for assessing translational potential and developing targeted interventions. Nevertheless, evaluating psilocybin's effects in a female model of RmTBI remains an important future direction.

In summary, our findings indicate that psilocybin may improve behavioural deficits following RmTBI, accompanied by changes in microglial density and neurogenesis. These findings support its therapeutic potential for chronic TBI and support future clinical trials to investigate this.

Declarations

Acknowledgement

This work was funded by the Canadian Institutes of Health Research (FRN 163015) and Michael Smith Health Research BC (SCH-2021-1888). The authors thank the USONA Institute Investigational Drug Supply Program for providing the psilocybin used.

Conflict of interest:

The authors declare no competing financial interests.

References

1. Mavroudis I, Ciobica A, Bejenariu AC, Dobrin RP, Apostu M, Dobrin I, et al. Cognitive Impairment following Mild Traumatic Brain Injury (mTBI): A Review. Medicina (B Aires). 2024;60:380.
2. Konrad C, Geburek AJ, Rist F, Blumenroth H, Fischer B, Husstedt I, et al. Long-term cognitive and emotional consequences of mild traumatic brain injury. Psychol Med. 2011;41:1197–1211.
3. Hiskens MI, Li KM, Schneiders AG, Fenning AS. Repetitive mild traumatic brain injury-induced neurodegeneration and inflammation is attenuated by acetyl-L-carnitine in a preclinical model. Front Pharmacol. 2023;14.
4. McKee AC, Cantu RC, Nowinski CJ, Hedley-Whyte ET, Gavett BE, Budson AE, et al. Chronic Traumatic Encephalopathy in Athletes: Progressive Tauopathy After Repetitive Head Injury. J Neuropathol Exp Neurol. 2009;68:709–735.
5. Gavett BE, Stern RA, Cantu RC, Nowinski CJ, McKee AC. Mild traumatic brain injury: A risk factor for neurodegeneration. Alzheimers Res Ther. 2010;2:1–3.
6. Dehbozorgi M, Maghsoudi MR, Rajai S, Mohammadi I, Nejad AR, Rafiei MA, et al. Depression after traumatic brain injury: A systematic review and Meta-analysis. Am J Emerg Med. 2024;86:21–29.
7. Loane DJ, Kumar A. Microglia in the TBI Brain: The Good, The Bad, And The Dysregulated. Exp Neurol. 2016;275:316.
8. Eyolfson E, Khan A, Mychasiuk R, Lohman AW. Microglia dynamics in adolescent traumatic brain injury. Journal of Neuroinflammation 2020 17:1. 2020;17:326-.
9. Green TRF, Rowe RK. Quantifying microglial morphology: an insight into function. Clin Exp Immunol. 2024;216:221–229.
10. Aungst SL, Kabadi S V., Thompson SM, Stoica BA, Faden AI. Repeated mild traumatic brain injury causes chronic neuroinflammation, changes in hippocampal synaptic plasticity, and associated cognitive deficits. Journal of Cerebral Blood Flow and Metabolism. 2014;34:1223–1232.
11. Wang J, Zhang B, Li L, Tang X, Zeng J, Song Y, et al. Repetitive traumatic brain injury–induced complement C1–related inflammation impairs long-term hippocampal neurogenesis. Neural Regen Res. 2025;20:821–835.
12. Bah TM, Yeturu SN, Samudrala N, Feller S, Bui B, Villasana L. Absence of the Neurogenic Response to a Repeated Concussive-Like Injury and Associated Deficits in Strategy Flexibility. J Neurotrauma.

2025;42:952–973.

13. Greer K, Basso EKG, Kelly C, Cash A, Kowalski E, Cerna S, et al. Abrogation of atypical neurogenesis and vascular-derived EphA4 prevents repeated mild TBI-induced learning and memory impairments. Sci Rep. 2020;10:15374-.
14. Gemma C, Bachstetter AD. The role of microglia in adult hippocampal neurogenesis. Front Cell Neurosci. 2013;7:46146.
15. Al-Onaizi M, Al-Khalifah A, Qasem D, Elali A. Role of Microglia in Modulating Adult Neurogenesis in Health and Neurodegeneration. Int J Mol Sci. 2020;21:6875.
16. Allen J, Dames SS, Foldi CJ, Shultz SR. Psychedelics for acquired brain injury: a review of molecular mechanisms and therapeutic potential. Molecular Psychiatry 2023. 2024:1–15.
17. Plummer Z, Allen J, Brand J, Mayo LM, Shultz SR, Christie BR. Examining the potential of psilocybin and 5-MeO-DMT as therapeutics for traumatic brain injury. Prog Neuropsychopharmacol Biol Psychiatry. 2025:111448.
18. Kit A, Conway K, Makarowski S, O'Regan G, Allen J, Shultz SR, et al. Can the gut-brain axis provide insight into psilocybin's therapeutic value in reducing stress? Neurobiol Stress. 2025:100732.
19. Meshkat S, Tello-Gerez TJ, Gholaminezhad F, Dunkley BT, Reichelt AC, Erritzoe D, et al. Impact of psilocybin on cognitive function: A systematic review. Psychiatry Clin Neurosci. 2024;78:744–764.
20. Doss MK, Považan M, Rosenberg MD, Sepeda ND, Davis AK, Finan PH, et al. Psilocybin therapy increases cognitive and neural flexibility in patients with major depressive disorder. Transl Psychiatry. 2021;11.
21. Schindler EAD. Psychedelics as preventive treatment in headache and chronic pain disorders. Neuropharmacology. 2022;215:109166.
22. Schindler EAD, Sewell RA, Gottschalk CH, Luddy C, Flynn LT, Lindsey H, et al. Exploratory Controlled Study of the Migraine-Suppressing Effects of Psilocybin. Neurotherapeutics. 2021;18:534–543.
23. Yasin B, Mehta S, Tewfik G, Bekker A. Psychedelics as novel therapeutic agents for chronic pain: mechanisms and future perspectives. Open Exploration 2019 3:5. 2024;3:418–433.
24. Natoli S, Cuomo A, Marchesini M, Luongo L, Lo Bianco G, Guardamagna VA, et al. Psilocybin and Chronic Pain: A New Perspective for Future Pain Therapists? Med Sci (Basel). 2025;13:277.
25. Johnson MW, Garcia-Romeu A, Griffiths RR. Long-term follow-up of psilocybin-facilitated smoking cessation. Am J Drug Alcohol Abuse. 2017;43:55–60.
26. Bogenschutz MP, Ross S, Bhatt S, Baron T, Forcehimes AA, Laska E, et al. Percentage of Heavy Drinking Days Following Psilocybin-Assisted Psychotherapy vs Placebo in the Treatment of Adult Patients With Alcohol Use Disorder: A Randomized Clinical Trial. JAMA Psychiatry. 2022. 24 August 2022. https://doi.org/10.1001/JAMAPSYCHIATRY.2022.2096.
27. van der Meer PB, Fuentes JJ, Kaptein AA, Schoones JW, de Waal MM, Goudriaan AE, et al. Therapeutic effect of psilocybin in addiction: A systematic review. Front Psychiatry. 2023;14:1134454.
28. Ly C, Greb AC, Vargas M V., Duim WC, Grodzki ACG, Lein PJ, et al. Transient Stimulation with Psychoplastogens Is Sufficient to Initiate Neuronal Growth. ACS Pharmacol Transl Sci. 2021;4:452–460.

29. Vargas M V., Dunlap LE, Dong C, Carter SJ, Tombari RJ, Jami SA, et al. Psychedelics promote neuroplasticity through the activation of intracellular 5-HT2A receptors. Science. 2023;379:700–706.
30. Ly C, Greb AC, Cameron LP, Wong JM, Barragan E V., Wilson PC, et al. Psychedelics Promote Structural and Functional Neural Plasticity. Cell Rep. 2018;23:3170.
31. Moliner R, Girych M, Brunello CA, Kovaleva V, Biojone C, Enkavi G, et al. Psychedelics promote plasticity by directly binding to BDNF receptor TrkB. Nat Neurosci. 2023;26:1032–1041.
32. Hesselgrave N, Troppoli TA, Wulff AB, Cole AB, Thompson SM. Harnessing psilocybin: Antidepressant-like behavioral and synaptic actions of psilocybin are independent of 5-HT2R activation in mice. Proc Natl Acad Sci U S A. 2021;118.
33. Shao LX, Liao C, Davoudian PA, Savalia NK, Jiang Q, Wojtasiewicz C, et al. Psilocybin's lasting action requires pyramidal cell types and 5-HT2A receptors. Nature. 2025;642:411–420.
34. Shao LX, Liao C, Gregg I, Davoudian PA, Savalia NK, Delagarza K, et al. Psilocybin induces rapid and persistent growth of dendritic spines in frontal cortex in vivo. Neuron. 2021;109:2535-2544.e4.
35. Zhao X, Du Y, Yao Y, Dai W, Yin Y, Wang G, et al. Psilocybin promotes neuroplasticity and induces rapid and sustained antidepressant-like effects in mice. Https://DoiOrg/101177/02698811241249436. 2024;38:489–499.
36. Catlow BJ, Song S, Paredes DA, Kirstein CL, Sanchez-Ramos J. Effects of psilocybin on hippocampal neurogenesis and extinction of trace fear conditioning. Exp Brain Res. 2013;228:481–491.
37. Laabi S, LeMmon C, Vogel C, Chacon M, Jimenez VM. Psilocybin and psilocin regulate microglial immunomodulation and support neuroplasticity via serotonergic and AhR signaling. Int Immunopharmacol. 2025;159:114940.
38. Wiens KR, Brooks NAH, Riar I, Greuel BK, Lindhout IA, Klegeris A. Psilocin, the Psychoactive Metabolite of Psilocybin, Modulates Select Neuroimmune Functions of Microglial Cells in a 5-HT2 Receptor-Dependent Manner. Molecules. 2024;29:5084.
39. Mason NL, Szabo A, Kuypers KPC, Mallaroni PA, de la Torre Fornell R, Reckweg JT, et al. Psilocybin induces acute and persisting alterations in immune status in healthy volunteers: An experimental, placebo-controlled study. Brain Behav Immun. 2023;114:299–310.
40. Smedfors G, Olson L, Karlsson T. Psilocybin Combines Rapid Synaptogenic And Anti-Inammatory Effects In Vitro. 2022. 2022. https://doi.org/10.21203/rs.3.rs-1321542/v1.
41. Kato K, Kleinhenz JM, Shin YJ, Coarfa C, Zarrabi AJ, Hecker L. Psilocybin treatment extends cellular lifespan and improves survival of aged mice. Npj Aging. 2025;11:1–7.
42. Sun M, Allen J, Baker TL, Spitz G, Xavier S, Lee N, et al. The chronic aftermath of recurrent intimate partner violence-related brain injuries: Insights from rat models of traumatic brain injury and non-fatal strangulation. Exp Neurol. 2025;In press.
43. Allen J, Sun M, Baker TL, Dames S, Kryskow P, Christie BR, et al. Psilocybin mitigates chronic behavioral and neurobiological alterations in a rat model of recurrent intimate partner violence-related brain injury. Molecular Psychiatry 2025. 2025:1–14.
44. Sun M, Symons GF, Spitz G, O'Brien WT, Baker TL, Fan J, et al. Pathophysiology, blood biomarkers, and functional deficits after intimate partner violence-related brain injury: Insights from emergency

department patients and a new rat model. Brain Behav Immun. 2025;123:383–396.

45. Meconi A, Wortman RC, Wright DK, Neale KJ, Clarkson M, Shultz SR, et al. Repeated mild traumatic brain injury can cause acute neurologic impairment without overt structural damage in juvenile rats. PLoS One. 2018;13.
46. Pham L, Shultz SR, Kim HA, Brady RD, Wortman RC, Genders SG, et al. Mild closed-head injury in conscious rats causes transient neurobehavioral and glial disturbances: A novel experimental model of concussion. J Neurotrauma. 2019;36:2260–2271.
47. Sun M, Brady RD, Casillas-Espinosa PM, Wright DK, Semple BD, Kim HA, et al. Aged rats have an altered immune response and worse outcomes after traumatic brain injury. Brain Behav Immun. 2019;80:536–550.
48. Sun M, Baker TL, Wilson CT, Brady RD, Yamakawa GR, Wright DK, et al. Treatment with the vascular endothelial growth factor-A antibody, bevacizumab, has sex-specific effects in a rat model of mild traumatic brain injury. Journal of Cerebral Blood Flow and Metabolism. 2023. 7 November 2023. https://doi.org/10.1177/0271678X231212377/ASSET/IMAGES/LARGE/10.1177_0271678X231212377-FIG6.JPEG.
49. Barlow KM, Ponsford JL, Theodom A, Cowen G, Davis GA, Anderson V, et al. Mild traumatic brain injury and concussion and persisting post-concussion symptoms: new guidelines to support evidence-based assessment and management in Australia and Aotearoa New Zealand. Med J Aust. 2025;223:446–449.
50. Hibicke M, Landry AN, Kramer HM, Talman ZK, Nichols CD. Psychedelics, but Not Ketamine, Produce Persistent Antidepressant-like Effects in a Rodent Experimental System for the Study of Depression. ACS Appl Mater Interfaces. 2020. 2020. https://doi.org/10.1021/ACSCHEMNEURO.9B00493/SUPPL_FILE/CN9B00493_LIVESLIDES.MP4.
51. Halberstadt AL, Geyer MA. Characterization of the head-twitch response induced by hallucinogens in mice: detection of the behavior based on the dynamics of head movement. Psychopharmacology (Berl). 2013;227:727–739.
52. Commons KG, Cholanians AB, Babb JA, Ehlinger DG. The Rodent Forced Swim Test Measures Stress-Coping Strategy, Not Depression-like Behavior. ACS Chem Neurosci. 2017;8:955–960.
53. Shultz SR, McDonald SJ, Corrigan F, Semple BD, Salberg S, Zamani A, et al. Clinical Relevance of Behavior Testing in Animal Models of Traumatic Brain Injury. Https://HomeLiebertpubCom/Neu. 2020;37:2381–2400.
54. Johnston JN, Allen J, Shkolnikov I, Sanchez-Lafuente CL, Reive BS, Scheil K, et al. Reelin rescues behavioral, electrophysiological, and molecular metrics of a chronic stress phenotype in a similar manner to ketamine. ENeuro. 2023:ENEURO.0106-23.2023.
55. Allen J, Romay-Tallon R, Mitchell MA, Brymer KJ, Johnston J, Sánchez-Lafuente CL, et al. Reelin has antidepressant-like effects after repeated or singular peripheral injections. Neuropharmacology. 2022:109043.
56. Hibicke M, Kramer HM, Nichols CD. A Single Administration of Psilocybin Persistently Rescues Cognitive Deficits Caused by Adolescent Chronic Restraint Stress Without Long-Term Changes in

Synaptic Protein Gene Expression in a Rat Experimental System with Translational Relevance to Depression. Https://HomeLiebertpubCom/Psymed. 2023;1:54–67.

57. Viano DC, Hamberger A, Bolouri H, Säljö A. Concussion in professional football: Animal model of brain injury - Part 15. Neurosurgery. 2009;64:1162–1173.
58. Collins SM, O'Connell CJ, Reeder EL, Norman S V., Lungani K, Gopalan P, et al. Altered Serotonin 2A (5-HT 2A) Receptor Signaling Underlies Mild TBI-Elicited Deficits in Social Dominance. Front Pharmacol. 2022;13.
59. Avcu P, Fortress AM, Fragale JE, Spiegler KM, Pang KCH. Anhedonia following mild traumatic brain injury in rats: A behavioral economic analysis of positive and negative reinforcement. Behavioural Brain Research. 2019;368:111913.
60. Agtarap SD, Campbell-Sills L, Jain S, Sun X, Dikmen S, Levin H, et al. Satisfaction with Life after Mild Traumatic Brain Injury: A TRACK-TBI Study. J Neurotrauma. 2020;38:546–554.
61. Piña IG, Timmer-Murillo SC, Larson CL, deRoon-Cassini TA, Tomas CW. Trajectories of anhedonia symptoms after traumatic injury. European Journal of Trauma and Dissociation. 2024;8.
62. Feuston JL, Marshall-Fricker CG, Piper AM. The social lives of individuals with traumatic brain injury. Conference on Human Factors in Computing Systems - Proceedings. 2017;2017-May:182–194.
63. Hernandez-Leon A, Escamilla-Orozco RI, Tabal-Robles AR, Martínez-Vargas D, Romero-Bautista L, Escamilla-Soto G, et al. Antidepressant- and anxiolytic-like activities and acute toxicity evaluation of the Psilocybe cubensis mushroom in experimental models in mice. J Ethnopharmacol. 2024;320.
64. Goodwin GM, Aaronson ST, Alvarez O, Atli M, Bennett JC, Croal M, et al. Single-dose psilocybin for a treatment-resistant episode of major depression: Impact on patient-reported depression severity, anxiety, function, and quality of life. J Affect Disord. 2023;327:120–127.
65. Swieczkowski D, Kwaśny A, Pruc M, Gaca Z, Szarpak L, Cubała WJ. Psilocybin-assisted psychotherapy as a rapid-acting treatment for cancer-related depression and anxiety: Evidence from a network meta-analysis. Int J Psychiatry Med. 2025. 2025. https://doi.org/10.1177/00912174251337572/SUPPL_FILE/SJ-PDF-1-IJP-10.1177_00912174251337572.PDF.
66. Carhart-Harris RL, Bolstridge M, Rucker J, Day CMJ, Erritzoe D, Kaelen M, et al. Psilocybin with psychological support for treatment-resistant depression: an open-label feasibility study. Lancet Psychiatry. 2016;0366:11–13.
67. Ross S, Bossis A, Guss J, Agin-Liebes G, Malone T, Cohen B, et al. Rapid and sustained symptom reduction following psilocybin treatment for anxiety and depression in patients with life-threatening cancer: A randomized controlled trial. Journal of Psychopharmacology. 2016;30:1165–1180.
68. Kelmendi B, Kichuk SA, DePalmer G, Maloney G, Ching THW, Belser A, et al. Single-dose psilocybin for treatment-resistant obsessive-compulsive disorder: A case report. Heliyon. 2022;8.
69. Vidal-Itriago A, Radford RAW, Aramideh JA, Maurel C, Scherer NM, Don EK, et al. Microglia morphophysiological diversity and its implications for the CNS. Front Immunol. 2022;13:997786.
70. Yang G, Xu X, Gao W, Wang X, Zhao Y, Xu Y. Microglia-orchestrated neuroinflammation and synaptic remodeling: roles of pro-inflammatory cytokines and receptors in neurodegeneration. Front Cell

Neurosci. 2025;19:1700692.

71. Turkin A, Tuchina O, Klempin F. Microglia Function on Precursor Cells in the Adult Hippocampus and Their Responsiveness to Serotonin Signaling. Front Cell Dev Biol. 2021;9:665739.
72. Krabbe G, Matyash V, Pannasch U, Mamer L, Boddeke HWGM, Kettenmann H. Activation of serotonin receptors promotes microglial injury-induced motility but attenuates phagocytic activity. Brain Behav Immun. 2012;26:419–428.
73. Segi-Nishida E, Suzuki K. Regulation of adult-born and mature neurons in stress response and antidepressant action in the dentate gyrus of the hippocampus. Neurosci Res. 2025;211:10–15.
74. Leschik J, Lutz B, Gentile A. Stress-Related Dysfunction of Adult Hippocampal Neurogenesis—An Attempt for Understanding Resilience? Int J Mol Sci. 2021;22:7339.
75. Toda T, Parylak SL, Linker SB, Gage FH. The role of adult hippocampal neurogenesis in brain health and disease. Mol Psychiatry. 2018;24:67.
76. McCorkle TA, Romm ZL, Raghupathi R. Repeated Mild TBI in Adolescent Rats Reveals Sex Differences in Acute and Chronic Behavioral Deficits. Neuroscience. 2022;493:52–68.
77. Weber ET, Andrade R. Htr2a Gene and 5-HT(2A) Receptor Expression in the Cerebral Cortex Studied Using Genetically Modified Mice. Front Neurosci. 2010;4.
78. Lima da Cruz RV, Moulin TC, Petiz LL, Leão RN. A Single Dose of 5-MeO-DMT Stimulates Cell Proliferation, Neuronal Survivability, Morphological and Functional Changes in Adult Mice Ventral Dentate Gyrus. Front Mol Neurosci. 2018;11:312.
79. Szabo A, Kovacs A, Riba J, Djurovic S, Rajnavolgyi E, Frecska E. The endogenous hallucinogen and trace amine N,N-dimethyltryptamine (DMT) displays potent protective effects against hypoxia via sigma-1 receptor activation in human primary iPSC-derived cortical neurons and microglia-like immune cells. Front Neurosci. 2016;10:423.
80. Kourrich S, Su TP, Fujimoto M, Bonci A. The sigma-1 receptor: Roles in neuronal plasticity and disease. Trends Neurosci. 2012;35:762–771.
81. Neale KJ, Reid HMO, Sousa B, McDonagh E, Morrison J, Shultz S, et al. Repeated mild traumatic brain injury causes sex-specific increases in cell proliferation and inflammation in juvenile rats. Journal of Neuroinflammation 2023 20:1. 2023;20:1–20.
82. Haynes N, Goodwin T. Literature Review of Sex Differences in mTBI. Mil Med. 2021. 13 November 2021. https://doi.org/10.1093/MILMED/USAB472.
83. Wright DK, Symons GF, O'Brien WT, McDonald SJ, Zamani A, Major B, et al. Diffusion Imaging Reveals Sex Differences in the White Matter following Sports-Related Concussion. Cerebral Cortex. 2021;31:4411–4419.
84. Kalimon OJ, Sullivan PG. Sex Differences in Mitochondrial Function Following a Controlled Cortical Impact Traumatic Brain Injury in Rodents. Front Mol Neurosci. 2021;14:753946.
85. Ferguson SA, Mouzon BC, Lynch C, Lungmus C, Morin A, Crynen G, et al. Negative impact of female sex on outcomes from repetitive mild traumatic brain injury in hTau mice is age dependent: A chronic effects of Neurotrauma Consortium study. Front Aging Neurosci. 2017;9.

86. Kirby ED, Andrushko JW, Boyd LA, Koschutnig K, D'Arcy RCN. Sex differences in patterns of white matter neuroplasticity after balance training in young adults. Front Hum Neurosci. 2024;18:1432830.
87. Hyer MM, Phillips LL, Neigh GN. Sex Differences in Synaptic Plasticity: Hormones and Beyond. Front Mol Neurosci. 2018;11:266.
88. Goel N, Bale TL. Sex Differences in the Serotonergic Influence on the Hypothalamic-Pituitary-Adrenal Stress Axis. Endocrinology. 2010;151:1784.

Tables

Table 1. Effects of RmTBI and psilocybin treatment on Cd11b-positive microglia.

Cd11b-mciroglia	RmTBI	Psilocybin	Interaction
Microglial counts	F(1, 33)=9.989, **p=0.003****	F(1, 33)=2.705, p=0.110	F(1, 33)=0.916, p=0.346
Soma area	F(1, 33)=1.125, p=0.296	F(1, 33)=2.953, p=0.095	F(1, 33)=4.420, **p=0.043***
Soma perimeter	F(1, 33)=1.220, p=0.277	F(1, 33)=3.460, p=0.072	F(1, 33)=2.923, p=0.096
Soma roundness	F(1, 33)=0.163, p=0.688	F(1, 33)=0.895, p=0.351	F(1, 33)=0.094, p=0.761
Process quantity	Kruskal-Wallis: H=8.583, **p=0.035***		
Process nodes	F(1, 33)=4.039, p=0.052	F(1, 33)=0.421, p=0.521	F(1, 33)=1.984, p=0.168
Process endings	F(1, 33)=5.651, **p=0.023***	F(1, 33)=0.320, p=0.575	F(1, 33)=2.002, p=0.166
Total process length	F(1, 33)=5.067, p=0.031	F(1, 33)=0.088, p=0.768	F(1, 33)=1.566, p=0.219
Process surface area	F(1, 33)=5.032, **p=0.031***	F(1, 33)=0.104, p=0.748	F(1, 33)=1.587, p=0.216
Process complexity	F(1, 33)=2.216, p=0.146	F(1, 33)=0.372, p=0.545	F(1, 33)=2.216, p=0.146
Sholl number of nodes 10 µm	F(1, 33)=2.043, p=0.162	F(1, 33)=0.979, p=0.330	F(1, 33)=2.720, p=0.109
Sholl number of nodes 20 µm	F(1, 33)=6.189, **p=0.018***	F(1, 33)=0.577, p=0.767	F(1, 33)=6.524, **p=0.015***
Sholl number of nodes 30 µm	F(1, 33)=0.226, p=0.638	F(1, 33)=0.585, p=0.450	F(1, 33)=1.732, p=0.197
Sholl number of nodes 40 µm	F(1, 33)=0.022, p=0.882	F(1, 33)=1.311, p=0.260	F(1, 33)=0.022, p=0.882
Sholl number of nodes 50 µm	Kruskal-Wallis: H=2.346, p=0.504		
Sholl number of endings 10 µm	F(1, 33)=3.646, p=0.065	F(1, 33)=0.594, p=0.446	F(1, 33)=1.222, p=0.277
Sholl number of endings 20 µm	F(1, 33)=6.795, **p=0.014***	F(1, 33)=1.803, p=0.188	F(1, 33)=0.156, p=0.695
Sholl number of endings 30 µm	F(1, 33)=1.203, p=0.281	F(1, 33)=1.101, p=0.302	F(1, 33)=3.548, p=0.068
Sholl number of endings 40 µm	Kruskal-Wallis: H=1.621, p=0.655		
Sholl number of endings 50 µm	F(1, 33)=2.889, p=0.099	F(1, 33)=2.123, p=0.155	F(1, 33)=0.001, p=0.999

Sholl process length 10 µm	F(1, 33)=9.195, **p=0.005****	F(1, 33)=0.023, p=0.880	F(1, 33)=0.036, p=0.851
Sholl process length 20 µm	F(1, 33)=3.863, p=0.058	F(1, 33)=0.152, p=0.699	F(1, 33)=1.714, p=0.200
Sholl process length 30 µm	F(1, 33)=0.595, p=0.446	F(1, 33)=0.090, p=0.767	F(1, 33)=3.012, p=0.092
Sholl process length 40 µm	F(1, 33)=1.861, p=0.182	F(1, 33)=1.210, p=0.279	F(1, 33)=0.026, p=0.874
Sholl process length 50 µm	Kruskal-Wallis: H=3.104, p=0.376		
Sholl number of intersections 10 µm	F(1, 33)=8.288, **p=0.007****	F(1, 33)=0.499, p=0.485	F(1, 33)=0.962, p=0.334
Sholl number of intersections 20 µm	F(1, 33)=1.006, p=0.323	F(1, 33)=0.276, p=0.603	F(1, 33)=1.918, p=0.175
Sholl number of intersections 30 µm	F(1, 33)=0.846, p=0.364	F(1, 33)=3.565, p=0.068	F(1, 33)=0.084, p=0.773
Sholl number of intersections 40 µm	Kruskal-Wallis: H=2.483, p=0.478		
Sholl number of intersections 50 µm	Kruskal-Wallis: H=0.480, p=0.923		

Table 2. Effects of RmTBI and psilocybin treatment on DCX-positive neurons.

DCX-positive neurons	RmTBI	Psilocybin	Interaction
Neuron counts	F(1, 26)=1.844, p=0.186	F(1, 26)=7.557, **p=0.011***	F(1, 26)=0.366, p=0.550
Soma area	F(1, 26)=0.021, p=0.885	F(1, 26)=1.326, p=0.260	F(1, 26)=0.057, p=0.813
Soma perimeter	F(1, 26)=0.019, p=0.893	F(1, 26)=0.458, p=0.504	F(1, 26)=0.044, p=0.836
Soma roundness	F(1, 26)=0.0004, p=0.984	F(1, 26)=0.128, p=0.723	F(1, 26)=0.757, p=0.392
Dendritic nodes	F(1, 26)=0.152, p=0.650	F(1, 26)=3.701, p=0.065	F(1, 26)=1.105, p=0.303
Dendritic endings	F(1, 26)=0.373, p=0.546	F(1, 26)=3.546, p=0.071	F(1, 26)=1.094, p=0.305
Dendrite length	F(1, 26)=0.592, p=0.449	F(1, 26)=6.217, **p=0.019***	F(1, 26)=0.595, p=0.447
Dendrite surface area	F(1, 26)=0.940, p=0.341	F(1, 26)=6.569, **p=0.017***	F(1, 26)=0.581, p=0.453
Dendrite complexity	Kruskal-Wallis: H=8.015, **p=0.046***		
Sholl nodes 10-30 µm	F(1, 26)=0.590, p=0.449	F(1, 26)=0.039, p=0.844	F(1, 26)=0.039, p=0.844
Sholl nodes 30-50 µm	F(1, 26)=1.145, p=0.295	F(1, 26)=0.038, p=0.846	F(1, 26)=4.929, **p=0.035***
Sholl nodes 50-70 µm	F(1, 26)=0.004, p=0.950	F(1, 26)=0.054, p=0.818	F(1, 26)=0.110, p=0.743
Sholl nodes 70-90 µm	F(1, 26)=1.130, p=0.297	F(1, 26)=0.898, p=0.352	F(1, 26)=6.821, **p=0.015***
Sholl nodes 90-110 µm	F(1, 26)=0.129, p=0.723	F(1, 26)=6.309, **p=0.019***	F(1, 26)=0.966, p=0.335
Sholl nodes 110-130 µm	F(1, 26)=0.068, p=0.796	F(1, 26)=9.433, **p=0.005****	F(1, 26)=0.013, p=0.912
Sholl nodes 130-150 µm	Kruskal-Wallis: H=2.729, p=0.435		
Sholl nodes 150-170 µm	Kruskal-Wallis: H=4.568, p=0.206		
Sholl nodes 170-190 µm	Kruskal-Wallis: H=1,965, p=0.580		
Sholl nodes 190-210 µm	Kruskal-Wallis: H=2.750, p=0.432		
Sholl nodes 210-230 µm	Kruskal-Wallis: H=3.286, p=0.350		
Sholl nodes 230-250 µm	No variability		
Sholl endings 10-30 µm	Kruskal-Wallis: H=1.765, p=0.623		

Sholl endings 30-50 µm	Kruskal-Wallis: H=1.520, p=0.678		
Sholl endings 50-70 µm	F(1, 26)=0.671, p=0.420	F(1, 26)=0.841, p=0.367	F(1, 26)=0.841, p=0.367
Sholl endings 70-90 µm	F(1, 26)=0.017, p=0.896	F(1, 26)=01.867, p=0.184	F(1, 26)=0.561, p=0.460
Sholl endings 90-110 µm	F(1, 26)=0.169, p=0.684	F(1, 26)=1.919, p=0.178	F(1, 26)=2.235, p=0.147
Sholl endings 110-130 µm	F(1, 26)=0.085, p=0.773	F(1, 26)=6.658, **p=0.016***	F(1, 26)=0.223, p=0.641
Sholl endings 130-150 µm	F(1, 26)=0.894, p=0.353	F(1, 26)=1.262, p=0.272	F(1, 26)=0.121, p=0.731
Sholl endings 150-170 µm	F(1, 26)=0.165, p=0.688	F(1, 26)=2.836, p=0.104	F(1, 26)=1.165, p=0.290
Sholl endings 170-190 µm	F(1, 26)=0.794, p=0.381	F(1, 26)=4.729, **p=0.039***	F(1, 26)=1.269, p=0.270
Sholl endings 190-210 µm	Kruskal-Wallis: H=1.529, p=0.678		
Sholl endings 210-230 µm	Kruskal-Wallis: H=1.681, p=0.641		
Sholl endings 230-250 µm	Kruskal-Wallis: H=7.483, p=0.058		
Sholl length 10-30 µm	F(1, 26)=0.223, p=0.641	F(1, 26)=0.077, p=0.784	F(1, 26)=0.113, p=0.740
Sholl length 30-50 µm	F(1, 26)=0.128, p=0.280	F(1, 26)=0.117, p=0.735	F(1, 26)=0.847, p=0.186
Sholl length 50-70 µm	F(1, 26)=0.195, p=0.662	F(1, 26)=0.365, p=0.551	F(1, 26)=2.204, p=0.150
Sholl length 70-90 µm	F(1, 26)=0.137, p=0.714	F(1, 26)=2.398, p=0.134	F(1, 26)=1.761, p=0.196
Sholl length 90-110 µm	F(1, 26)=0.951, p=0.338	F(1, 26)=7.396, **p=0.011***	F(1, 26)=0.539, p=0.470
Sholl length 110-130 µm	F(1, 26)=0.056, p=0.816	F(1, 26)=7.275, **p=0.012***	F(1, 26)=0.030, p=0.864
Sholl length 130-150 µm	F(1, 26)=0.007, p=0.936	F(1, 26)=3.666, p=0.067	F(1, 26)=0.013, p=0.911
Sholl length 150-170 µm	F(1, 26)=0.041, p=0.840	F(1, 26)=4.318, **p=0.048***	F(1, 26)=0.057, p=0.813
Sholl length 170-190 µm	F(1, 26)=0.419, p=0.523	F(1, 26)=1.724, p=0.201	F(1, 26)=0.018, p=0.894
Sholl length 190-210 µm	F(1, 26)=1.585, p=0.219	F(1, 26)=0.227, p=0.637	F(1, 26)=0.430, p=0.518
Sholl length 210-230 µm	Kruskal-Wallis: H=1.788, p=0.618		

Sholl length 230-250 µm	Kruskal-Wallis: H=1.777, p=0.620		
Sholl intersections 10-30 µm	F(1, 26)=0.975, p=0.332	F(1, 26)=3.705, p=0.409	F(1, 26)=0.022, p=0.883
Sholl intersections 30-50 µm	F(1, 26)=1.662, p=0.209	F(1, 26)=0.280, p=0.602	F(1, 26)=4.200, p=0.051
Sholl intersections 50-70 µm	F(1, 26)=0.071, p=0.792	F(1, 26)=0.460, p=0.504	F(1, 26)=2.289, p=0.142
Sholl intersections 70-90 µm	F(1, 26)=0.262, p=0.613	F(1, 26)=4.166, p=0.052	F(1, 26)=2.329, p=0.139
Sholl intersections 90-110 µm	F(1, 26)=0.809, p=0.377	F(1, 26)=7.060, **p=0.013***	F(1, 26)=0.142, p=0.709
Sholl intersections 110-130 µm	F(1, 26)=0.045, p=0.833	F(1, 26)=6.481, **p=0.017***	F(1, 26)=0.118, p=0.734
Sholl intersections 130-150 µm	F(1, 26)=0.008, p=0.931	F(1, 26)=3.214, p=0.085	F(1, 26)=0.039, p=0.844
Sholl intersections 150-170 µm	F(1, 26)=0.138, p=0.714	F(1, 26)=3.465, p=0.074	F(1, 26)=0.176, p=0.678
Sholl intersections 170-190 µm	F(1, 26)=0.754, p=0.393	F(1, 26)=0.735, p=0.399	F(1, 26)=0.0002, p=0.987
Sholl intersections 190-210 µm	F(1, 26)=1.688, p=0.205	F(1, 26)=0.086, p=0.772	F(1, 26)=0.417, p=0.524
Sholl intersections 210-230 µm	Kruskal-Wallis: H=2.879, p=0.411		
Sholl intersections 230-250 µm	Kruskal-Wallis: H=2.298, p=0.513		

Figures

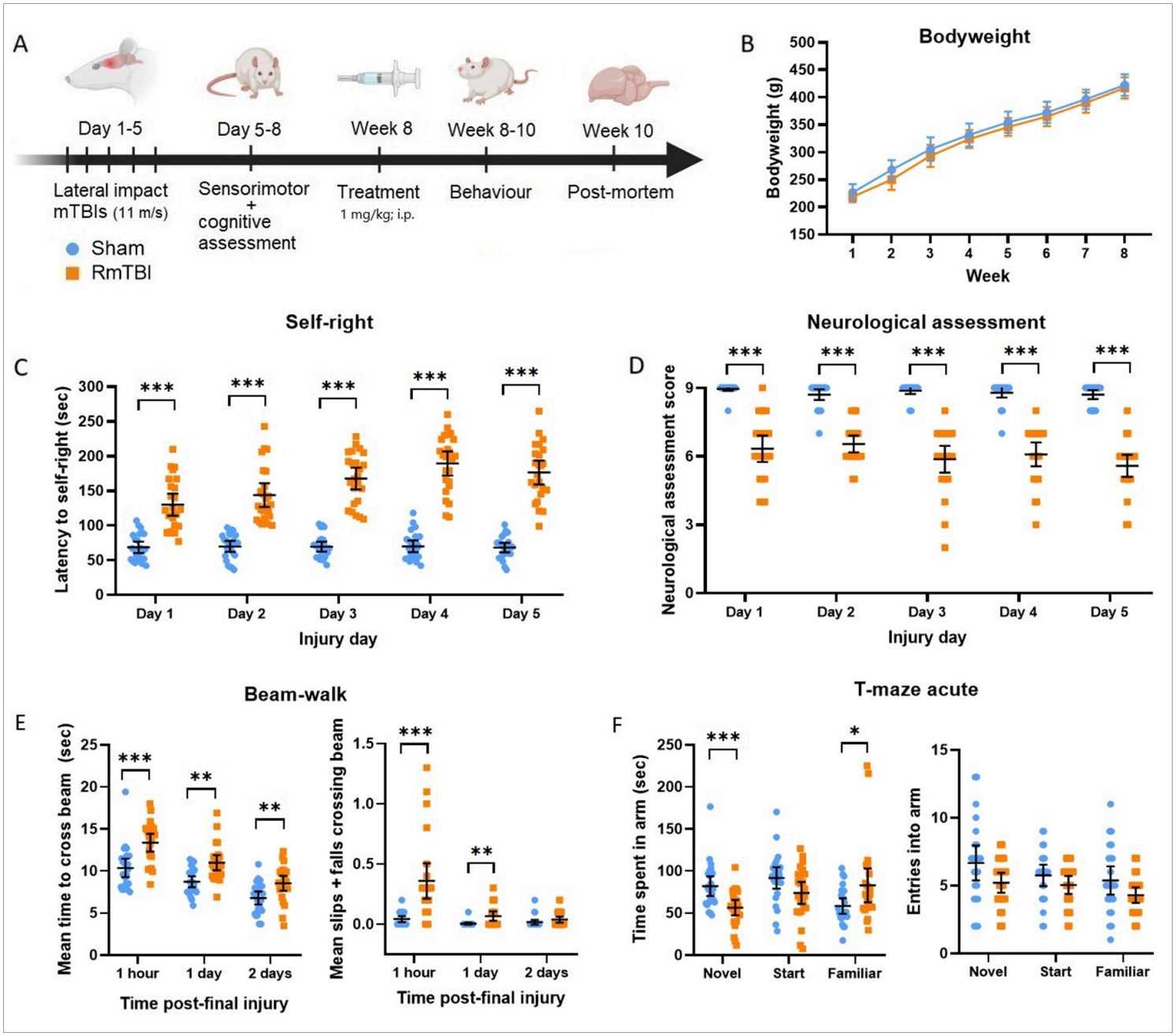

Figure 1

Experimetnal design and acute injury severity measures. A) Experimental design: male rats were subjected to five mild traumatic brain injuries given one day apart, followed by an 8 week recovery period, then psilocybin administration, then behavioural testing. **B)** RmTBI had no effect on bodyweight. **C)** RmTBI rats took longer to self-right after each injury. **D)** RmTBI rats performed poorer in the neurological assessments after each injury. **E)** RmTBI rats perfomred poorer in the beam-walk task 1 hr, 1 day, and 2 days post-final injury. **F)** RmTBI impaired spatial memory in the T-maze test. Data is presented as mean ± 95% confidence interval.*p<0.05/**p<0.01/***p<0.001 RmTBI effect.

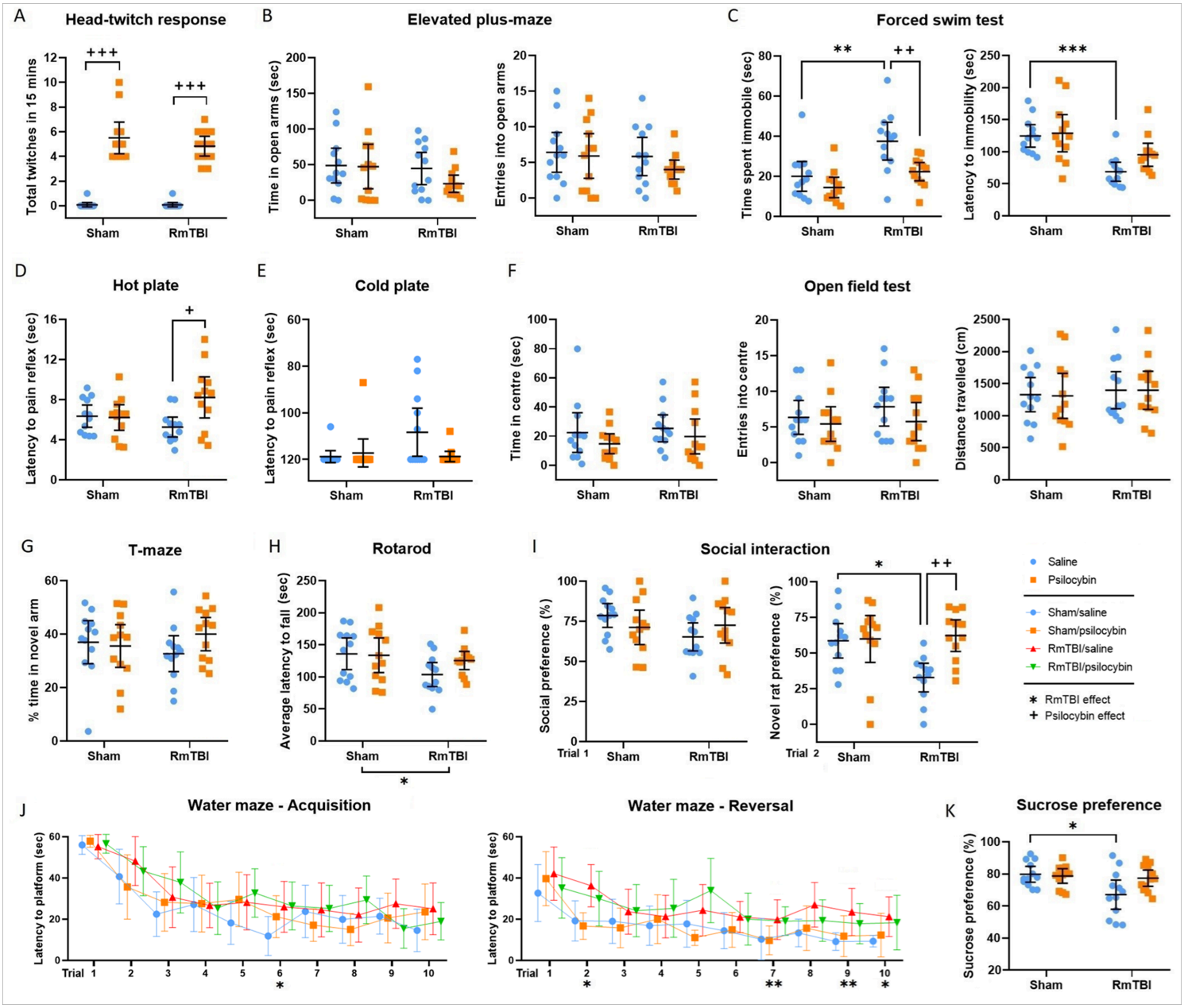

Figure 2

The effects of RmTBI and psilocybin on behaviour and cognition. A) Psilocybin elicited head-twitch responses in both sham and RmTBI rats, consistent with 5-HT_{2A} receptor activation. **B)** No significant effects of RmTBI or psilocybin were observed in the elevated plus-maze. **C)** Psilocybin attenuated RmTBI-induced increases in immobility in the forced swim test, indicating potential antidepressant-like effects. **D)** Psilocybin significantly increased reaction latency in the hot plate test, suggesting altered nociceptive processing. **E)** No significant effects of RmTBI or psilocybin were found in the cold plate test. **F)** Open field activity was unaffected by either RmTBI or psilocybin. **G)** Spatial memory in the T-maze was not significantly influenced by RmTBI or psilocybin. **H)** There were no effects of RmTBI or psilocybin in the Rotarod test. **I)** Psilocybin mitigated deficits in novel rat preference induced by RmTBI. **J)** RmTBI impaired spatial learning in both the acquisition and reversal phases of the water maze, reflected by longer platform search times. **K)** RmTBI decreased sucrose preference, suggesting anhedonia, in saline-treated rats. Data is presented as

mean ± 95% confidence interval. *p<0.05/**p<0.01/***p<0.001 RmTBI effect; +p<0.05/++p<0.01/+++p<0.001 psilocybin treatment effect.

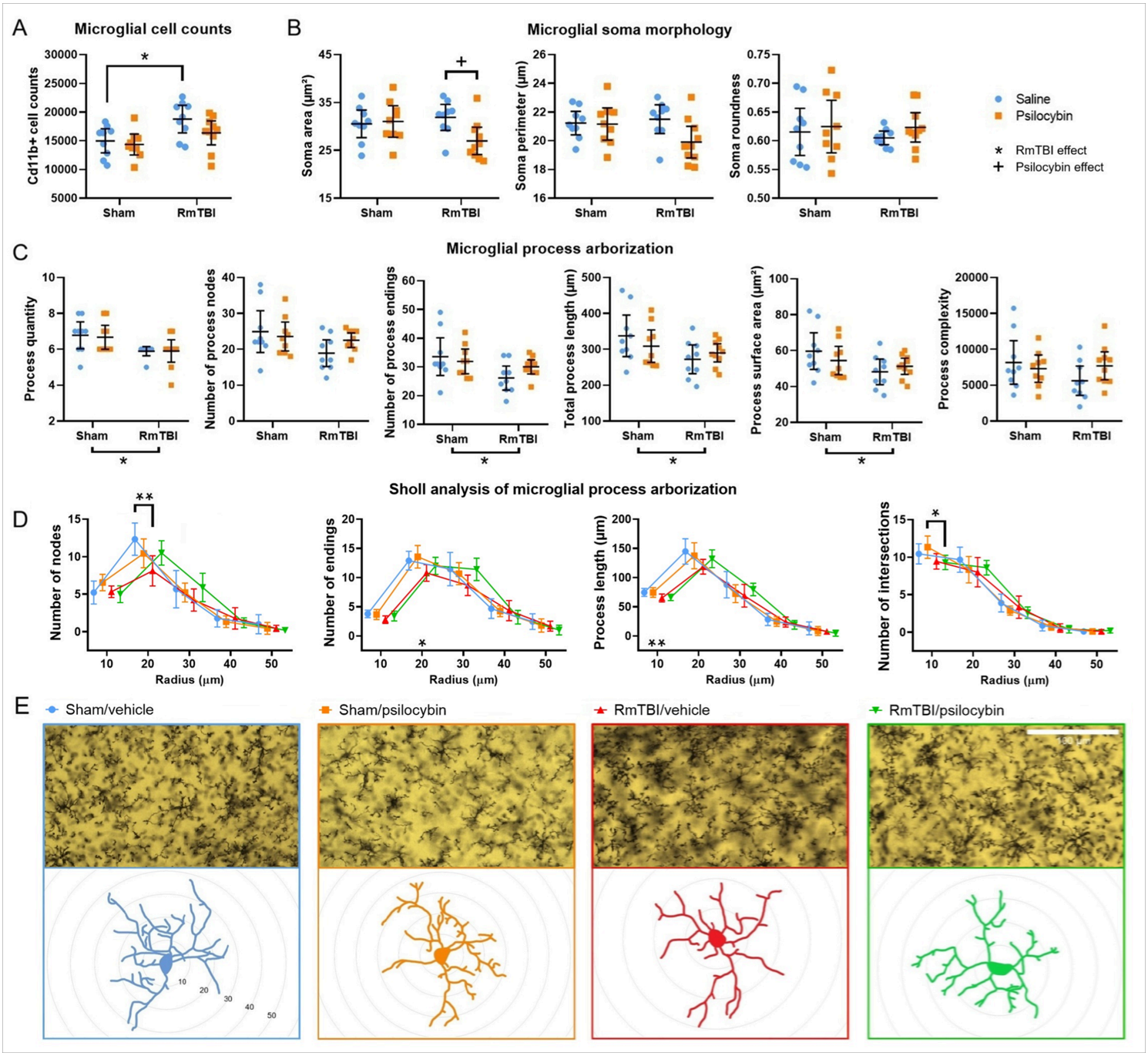

Figure 3

Effects of RmTBI and psilocybin on Cd11b-positive microglial counts and morphology. A) RmTBI increased Cd11b-positive microglial counts in the absence of psilocybin. **B)** Psilocybin reduced soma area in RmTBI rats. **C)** RmTBI decreased microglial process arborization. **D)** Sholl analysis revealed that RmTBI decreased the number of process nodes, the number of process endings, process length, and the number of Sholl intersections. **E)** Representative photomicrographs of Cd11b-positive microglia in the hippocampal molecular layer and representative microglial tracings. Data is presented as mean ± 95% confidence interval. *p<0.05/**p<0.01 RmTBI effect; +p<0.05 psilocybin treatment effect. Scale bar = 100 µm.

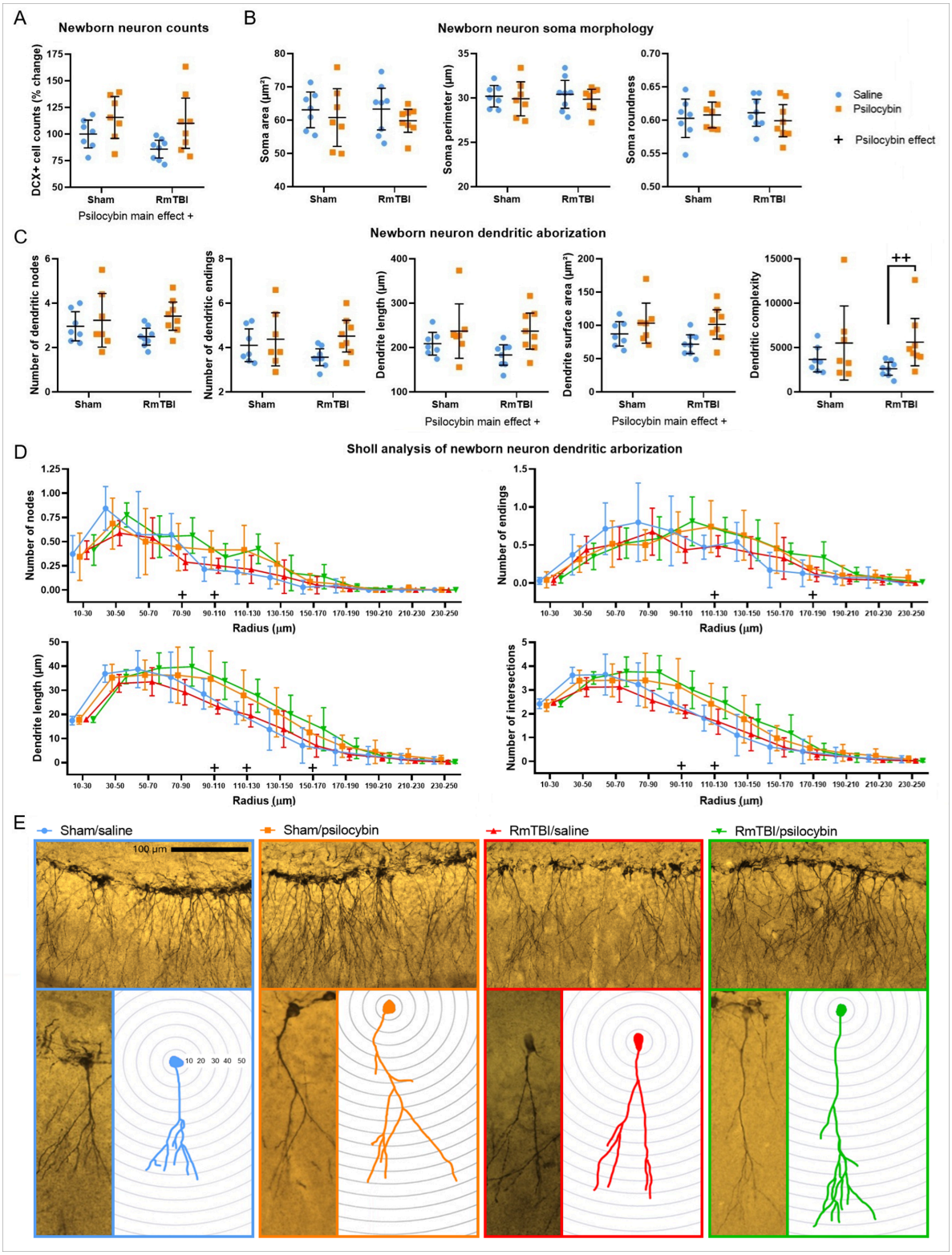

Figure 4

Effects of RmTBI and psilocybin on DCX-positive neuron counts and morphology. A) Psilocybin increased DCX-positive neuron profile counts. **B)** There was no effect of RmTBI or psilocybin on soma morphology. **C)** Psilocybin increased dendritic maturation. **D)**Sholl analysis revealed RmTBI had no effect on dendritic arborization across several radial segments, but psilocybin treatment increased the number of dendritic nodes, the number of dendritic endings, dendrite length, and the number of Sholl intersections. **E)**

Representative photomicrographs of DCX-positive neurons in the dentate granule cell layer and subgranular zone and corresponding tracings. Data is presented as mean ± 95% confidence interval. +p<0.05/++p<0.01 psilocybin treatment effect. Scale bar = 100 μm.